



OPEN

Advanced smart assistance with enhancing social interaction and daily activities for visually impaired individuals using deep learning with modified seagull optimization

Sana Alazwari¹✉, Hussah Nasser AlEisa², Mohammed Rizwanullah^{3,4} & Radwa Marzouk⁵

Visually impaired individuals face daily challenges in social engagement and routine activities due to limited access to real-time environmental information. Damage detection is a common approach in infrastructure that combines steel and concrete reinforcement to achieve optimal durability and structural strength. These bridges, designed to withstand diverse loads such as seismic forces, traffic weight, and environmental factors, are significant for maintaining structural integrity. Damage detection comprises applying advanced structural health monitoring methods to identify and assess potential deterioration or damage in concrete bridge components. Machine learning (ML) models, pattern detection, and statistical analysis are extensively adopted to identify subtle changes and process sensor information in structural response that might indicate corrosion, cracks, or other structural problems. Earlier detection and continuous monitoring of damage enable prompt intervention, ensuring longevity and safety while reducing the need for extensive repairs or the risk of unexpected failures. This study proposes an Automated Damage Detection using a Modified Seagull Optimizer with Ensemble Learning (ADD-MSGOEL) method for visually impaired people. The ADD-MSGOEL method is designed to enhance the social life and daily functioning of visually impaired people by accurately detecting damage and potential hazards in their surroundings. Initially, the ADD-MSGOEL method utilizes contrast enhancement (CLAHE) to enhance the image quality. Next, the features are extracted using the Dilated Convolution Block Attention Module with EfficientNet (DCBAM-EfficientNet) module, which derives the intrinsic and complex features. Moreover, the MSGO model is employed to choose the optimal parameter for the DCBAM-EfficientNet module. At last, an ensemble of three models, namely long short-term memory (LSTM), bidirectional gated recurrent unit (BiGRU), and sparse autoencoder (SAE) models, are implemented for the classification and detection of the damages. To demonstrate the effectiveness of the ADD-MSGOEL technique, a series of experiments were conducted using the CODEBRIM dataset. The experimental validation of the ADD-MSGOEL technique portrayed a superior accuracy value of 97.59% over existing models.

Keywords Damage detection, Visually impaired people, Social life and daily activities, CLAHE, Ensemble learning, Seagull optimizer

For visually impaired people, navigating social life and daily tasks is challenging due to barriers in perceiving environmental hazards or obstacles. The classification of basic injury in damage detection is a research area that has attracted significant attention for many years. The main motive for its flow in reputation is an old road and rail structure exposed to traffic loading states that far best novel design measures¹. This extraordinary upsurge in loading quickens fundamental fatigue and decreases service life. Furthermore, as bridge structures endure and

¹Department of Information Technology, College of Computers and Information Technology, Taif University, P.O. Box 11099, Taif 21944, Saudi Arabia. ²Department of Computer Sciences, College of Computer and Information Sciences, Princess Nourah bint Abdulrahman University, Riyadh, Saudi Arabia. ³Department of Computer and Self Development, Preparatory Year Deanship, Prince Sattam bin Abdulaziz University, AlKharj, Saudi Arabia. ⁴King Salman Center for Disability Research, Riyadh 11614, Saudi Arabia. ⁵Department of Mathematics, Faculty of Science, Cairo University, Giza 12613, Egypt. ✉email: alazwari.s@tu.edu.sa

weaken, the examination frequency should be enhanced to respond to the decrease in the protection of these structures². Damage detection is the main highway of the infrastructure system, which has been aimed to aid for an extended period. However, faults might drop at the time when the bridge was planned. Generally, the visual examination of damage detection depends upon the engineers' view and knowledge³. Many engineers frequently face problems in checking parts that are complex to attain. As an outcome, mistakes and incorrect estimations of the bridge state valuation might occur. Due to this reason, numerous studies discussed the advanced application of non-destructive models incorporating artificial intelligence (AI) for state valuation⁴. In the present scenario, many efficient models and information technology (IT) methods become familiar and advanced enough to discover the problems around structural harm⁵. Numerous well-known innovative models accompanied by AI models have been found in structural damage recognition⁶. Artificial Neural Network (ANN) applications were performed in structural damage recognition and classification research before the deep learning (DL) model became commonly recognized. Several researchers have tried to create dissimilar models to enhance system identification excellence⁷. These works typically depend on handcrafted removing low-dimensional features and classical ML models. So, these techniques are primarily time-consuming tasks and may not be adequate, considering that faults in real conditions are complex with unavoidable background noise⁸. In recent years, attention has been paid to data-driven damage classification methods utilizing great ML models. DL approaches have gained significant attention among various ML techniques due to their high efficiency and accuracy in object recognition and classification⁹. Convolutional Neural Networks (CNN) were effectively confirmed to evaluate the definite number of structural damage over image detection. Also, these new technologies enhance damage recognition, such as the Internet of Things (IoT), which improves the timeliness and accuracy of observing data in Structural Health Monitoring¹⁰. Likewise, hazard classification in buildings might benefit from more vivid visualization technologies, e.g. Augmented Reality and Virtual Reality.

This study proposes an Automated Damage Detection using a Modified Seagull Optimizer with Ensemble Learning (ADD-MSGOEL) method for visually impaired people. The ADD-MSGOEL method is designed to enhance the social life and daily functioning of visually impaired people by accurately detecting damage and potential hazards in their surroundings. Initially, the ADD-MSGOEL method utilizes contrast enhancement (CLAHE) to enhance the image quality. Next, the features are extracted using the Dilated Convolution Block Attention Module with EfficientNet (DCBAM-EfficientNet) module, which derives the intrinsic and complex features. Moreover, the MSGO model is employed to choose the optimal parameter for the DCBAM-EfficientNet module. At last, an ensemble of three models, namely long short-term memory (LSTM), bidirectional gated recurrent unit (BiGRU), and sparse autoencoder (SAE) models, are implemented for the classification and detection of the damages. To demonstrate the effectiveness of the ADD-MSGOEL technique, a series of experiments were conducted using the CODEBRIM dataset. The key contribution of the ADD-MSGOEL technique is listed below.

- The CLAHE-based pre-processing improves the contrast and quality of input images, revealing subtle features that might otherwise be missed. This improvement allows the feature extraction process to concentrate on more relevant patterns, resulting in improved model performance. It plays a significant role in ensuring accurate and reliable damage detection in the system.
- The DCBAM-EfficientNet-based feature extraction employs dilated convolutions and attention mechanisms, improving the model's capability to capture complex patterns in the data. Incorporating these techniques with EfficientNet optimizes computational efficiency while maintaining high feature representation quality. This methodology significantly improves the model's capability to detect and classify damage accurately.
- The ensemble of LSTM, BiGRU, and SAE models integrates the unique merits of each architecture, ensuring robust damage classification and detection. This integration enhances accuracy and model generalization, allowing the system to handle diverse and complex data patterns better. The synergy between these models improves the overall performance of damage detection tasks.
- The MSGO approach is utilized for hyperparameter tuning, refining the model's efficiency and precision in predicting damage. This optimization technique improves the model's capability to fine-tune critical parameters, resulting in more accurate and reliable predictions. The model becomes more appropriate for complex damage detection tasks by improving hyperparameter selection.
- Integrating CLAHE-based pre-processing, DCBAM-EfficientNet feature extraction, and an ensemble of advanced models with MSGO-based tuning presents a novel approach to damage detection. This unique integration improves the model's accuracy and computational efficiency. Employing cutting-edge techniques such as attention mechanisms and optimized hyperparameters gives a more robust and reliable solution for real-time damage detection in complex environments.

Related works

Asghari et al.¹¹ developed an innovative deep ensemble learning (DEL) technique that relied on stacked simplification to identify damages during physical health monitoring. A distinctive feature of the developed method was deploying a multi-headed deep ANN (DANN) framework for classification complexity, with an NN as a meta-learner. In¹², a self-adaptive three-tier technique was presented. The primary system offers a recently designed segmentation system that implements a multi-objective aggressive weed optimizer and information theory-based form of images. Next, discrete wavelet transforms (DWT) and singular value decomposition are incorporated. The final system was designed to configure a rated spalling severity model dependent on depth and area. Hong et al.¹³ examined a present technique and developed an innovative system of integration training by bridge members. A DL-based super-resolution component has also been utilized. A DL integration model, dependent upon individual training via bridge members, was developed for efficiency upgrading and optimization. In¹⁴, a stacked ensemble learning method was introduced. Five unrelated heterogeneous ML

methods have been trained to forecast everyday occurrences; every system employed the contextual data's principal components analysis (PCA) as the input parameter. Then, a stacked ensemble learning was made using the outputs of the five individual systems. Lastly, a damage indicator integrating the forecast residuals of numerous natural occurrences was developed. Zhang et al.¹⁵ examined a vision-based crack identification technique for concrete bridge decks, combining 1D-CNN and LSTM techniques. At a pre-processing stage, images could be initially changed into the frequency domain to increase the training effectiveness. The method was also computed employing the flattened frequency data. LSTM was utilized to improve the effectiveness of the designed network.

In¹⁶, the efficiency of an innovative damage detection technique depends upon incorporating two signal processing methods that must achieve the ensemble empirical mode decomposition with modified noises, and numerous signal classification (CEEMDAN-MUSIC) methods were examined. Besides, the MUSIC technique could be implemented for the primary IMF of the processed signal. Laxman et al.¹⁷ designed an extensive automatic crack identification and crack depth estimation architecture for existing configurations employing images captured at portable devices. Primarily, a binary class CNN technique was introduced. In addition, a combined CNN method with convolutional feature extraction layer and regression techniques (XGBoost and RF) has been designed to forecast the depth of the cracks automatically. In¹⁸, a supervised DL method for damage recognition in bridge architectures was presented. The technique utilizes a hybrid system that integrates Finite Component outcomes to enhance the training stage of a DNN with synthetic damage states. The NN depended on AE, and its specific model permits the activating or deactivating of nonlinear relationships on the requirement. Atitallah et al.¹⁹ examine an obstacle detection method that depends on a modified YOLOv5 NN structure. The recommended method of identifying and detecting a fixed landmark outdoor and indoor objects is enormously valuable for Blind and Visually Impaired (BVI) navigation supports. In²⁰, an improved YOLO v8 method is efficaciously presented and specially intended for high-voltage power line damage detection. This method enhances strength and accuracy by introducing an adaptive threshold model, the GSConv convolutional network, and a lightweight network model, Slim Neck, but diminishing the model complexity.

The proposed method

In this study, the ADD-MSGOEL approach for visually impaired people is proposed. The ADD-MSGOEL approach is designed to enhance the social life and daily functioning of visually impaired people by accurately detecting damage and potential hazards in their surroundings. To accomplish that, the ADD-MSGOEL technique comprises different sub-processes, image enhancement, DCBAM-EfficientNet-based feature extractor, MSGO-based parameter tuning, and ensemble learning process. Figure 1 represents the entire flow of the presented ADD-MSGOEL technique.

Image enhancement

At the primary stage, the ADD-MSGOEL technique follows a based CLAHE approach to improve image qualities²¹. This model is chosen because it enhances the images' local contrast. It is beneficial for tasks involving image features that may be difficult to distinguish due to low contrast. Unlike conventional histogram equalization, CLAHE prevents over-amplification of noise by restricting the CLAHE in homogenous regions, making it ideal for improving the visibility of crucial features while preserving the overall structure of the image. This technique is advantageous in medical imaging, satellite imagery, or any context where subtle details are critical. Additionally, CLAHE adapts to diverse areas of an image, enhancing feature visibility across various lighting conditions and improving accuracy for subsequent model training compared to global techniques. Figure 2 specifies the structure of the CLAHE model.

An image-enhancing method, CLAHE, improves the novel image appearance and data value before processing. This technique is used to enhance the image visibility. CLAHE is a modified section of the Adaptive Histogram Equalization (AHE) procedure. In CLAHE, the image contrast is amended by executing CLHE to tiny data areas named tiles. Then, the resultant adjacent tiles are perfectly fused back using bi-linear interpolation. CLAHE is mainly used for grey-scale retinal images. The clip limit function will be more beneficial in limiting noise in the image. In the background area, pixel numbers have been separated similarly at every grey level; thus, the average pixel number is grey as below:

$$n_{avg} = \frac{n_{CR-x_p} * n_{CR-y_p}}{n_{gray}} \quad (1)$$

Whereas, n_{avg} refers to the number of the average pixels, n_{gray} signifies the amount of gray level, n_{CR-x_p} and n_{CR-y_p} denotes the number of pixels in the x and y direction, respectively.

After that, compute the actual clip limit.

$$n_{CL} = n_{CLIP} * n_{avg} \quad (2)$$

CLAHE is a valuable model in the bio-medical image process because it is highly effective at creating standard vital significant sections.

Illumination correction: This pre-processing model's primary goal is to decrease the state effect initiated by the uneven illumination of the retinal image. Each pixel strength is computed utilizing the expression as below:

$$p' = p + \mu_D - \mu_L \quad (3)$$

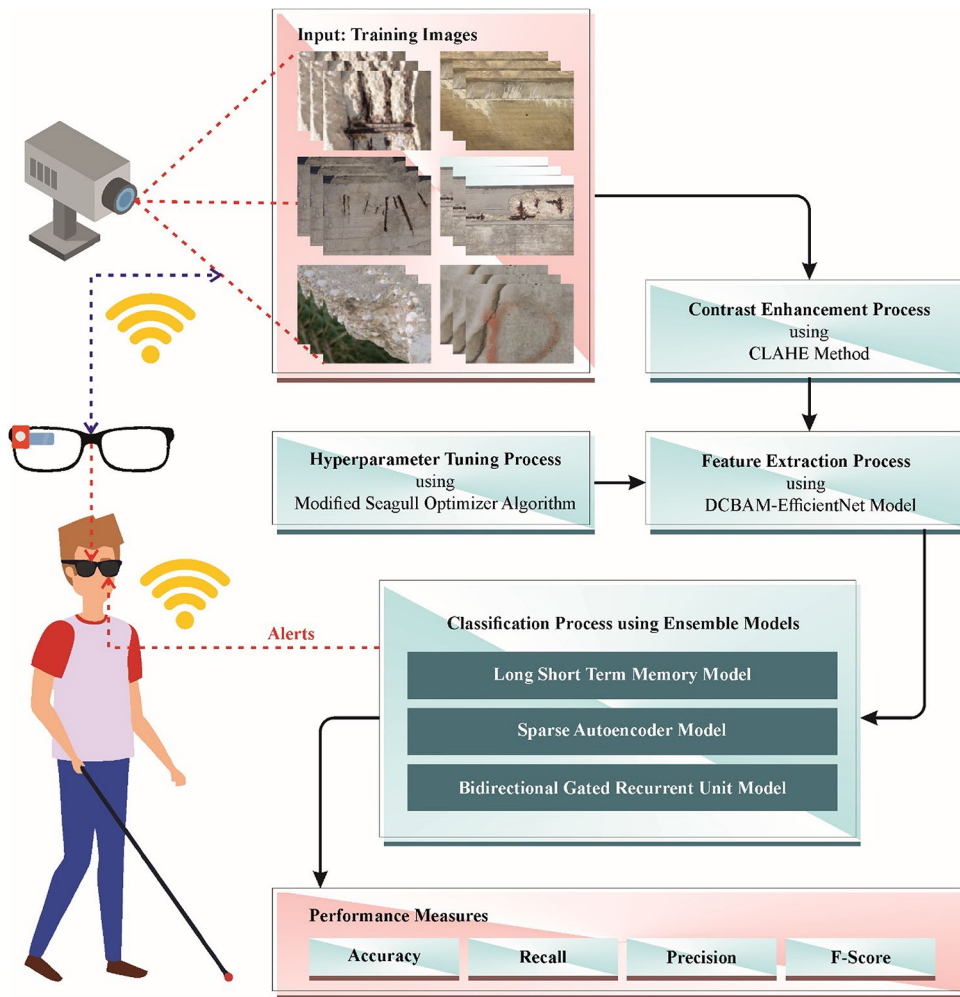


Fig. 1. Overall flow of ADD-MSGOEI approach.

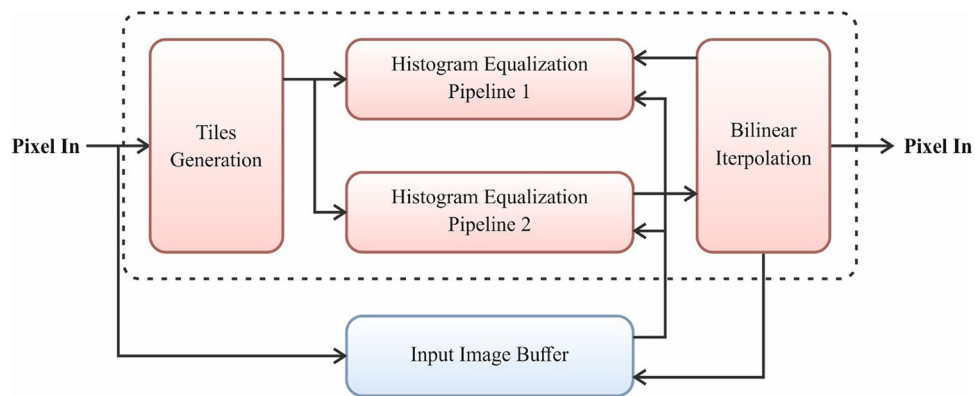


Fig. 2. CLAHE architecture.

Whereas μ_D and μ_L signify the desired and local average intensity, respectively. p' and p denote the latest and initial pixel size values correspondingly. This technique has improved microaneurysms at the retina surface.

Feature extraction

This work extracts the features using the DCBAM-EfficientNet Module, which derives the complex and intrinsic features²². This model integrates the merits of dilated convolutions, attention mechanisms, and EfficientNet for more effectual feature learning. Dilated convolutions capture multi-scale contextual data without losing

resolution, while the attention mechanism allows the model to concentrate on the most crucial features in the input. EfficientNet, known for its superior performance with fewer parameters, gives a lightweight yet robust backbone for feature extraction. This hybrid methodology improves the capability of the model to detect complex data patterns, enhancing accuracy and computational efficiency compared to conventional CNNs. Moreover, it addresses overfitting and underfitting, making it more robust for complex damage detection tasks. Figure 3 indicates the DCBAM-EfficientNet framework.

The network size is usually constrained by three sizes: input image resolution, channel amount, and network depth. In EfficientNet, a model multiple scaling technique has been developed to balance the three sizes, which are fully intended by a fixed scale factor and have numerous benefits. EfficientNet is a stacked Mobile Inverted Bottleneck Convolution (MBConv). Every module of MBConv contains an SE attention module, which compacts the input features to acquire the $1D$ features. Then, every channel weight is considered over the full connection layer, and lastly, it is multiplied by the element with the early feature map to achieve the weight task in the channel aspect.

The Convolution Block Attention Model (CBAM) is a lightweight and effectual unit that contains dual sub-modules, namely SAM (Spatial Attention Model) and CAM (Channel Attention Model). The SAM pays attention to the location data, input image compression, and pooling to procedure effective feature descriptors. CAM considers the significant content, reduces the input image, and groups the spatial data of the feature map utilizing global maximum and average pooling to produce channel attention. When equated with SE, CBAM has more impact on the location data and is adaptably embedded into the neural network to enhance the feature symbol ability without inserting significant overhead.

Assume a feature map $F \in R^{C \times H \times W}$ as input, it is initially handled by global average and highest pooling to attain dual dissimilar spatial feature descriptors F_{avg}^C and F_{max}^C , representing average and maximum pooling features correspondingly, with size $R^{C \times 1 \times 1}$. Then, they pass over the MLP unit, where the network amount is compacted to $1/r$ times and then extended to the unique number of channels. The dual is totalled element-wise after the ReLu function to produce the channel attention $M_C \in R^{C \times 1 \times 1}$ data. Element with input F increases the channel attention to attain adaptive feature map $F_1 \in R^{C \times H \times W}$. As exposed in Eqs. (4), (5).

$$\begin{aligned} M_C(F) &= \sigma(MLP(AvgPool(F)) + MLP(MaxPool(F))) \\ &= \sigma(W_1(F_{avg}^c) + W_1(F_{max}^c)) \end{aligned} \quad (4)$$

$$F_1 = M_C(F) \otimes F \quad (5)$$

Whereas σ refers to the function of the sigmoid, W_0 , W_1 denotes the MLP module weight and \otimes signifies the consistent element-wise multiplication.

Then, F_1 is selected as an input, and global average and maximum pooling are implemented to get dual-size vector $R^{1 \times H \times W}$. The vector is then merged and exposed to a 7×7 convolution process. The final spatial attention $M_S \in R^{1 \times H \times W}$ is exposed in Eqs. (6), (7).

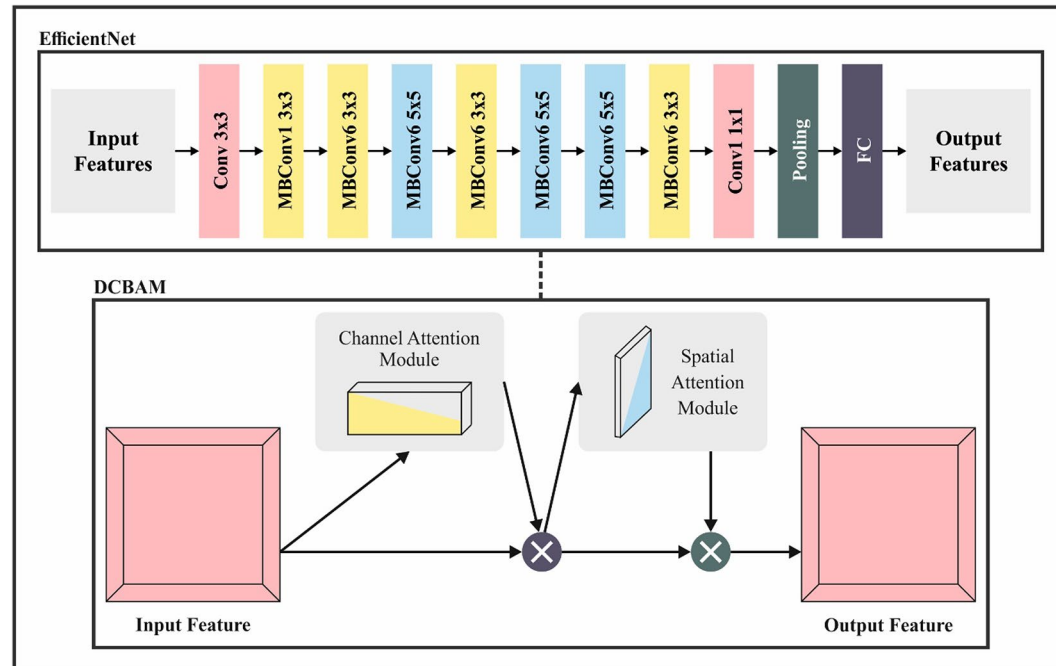


Fig. 3. DCBAM-EfficientNet framework.

$$M_s(F) = \sigma(f^{7 \times 7}([A \nu gPool(F); MaxPool(F)])) = \sigma(f^{7 \times 7}[F_{avg}^S; F_{max}^S]) \quad (6)$$

$$F_2 = M_S(F_1) \otimes F_1 \quad (7)$$

Whereas $f^{7 \times 7}$ denotes the 7×7 convolution operation

The convolution (Conv) operation size defines the receptive field range. The 7×7 Conv kernels in SAM to remove spatial features, equated to the usage of small 3×3 Conv kernels, upsurges the receptive field and enhances the number of parameters, which certainly restricts the use of CBAM. To manage this issue, this study replaces the complexity of the SAM in the CBAM with the enlarged convolution to diminish the number of models.

The input feature map $F \in R^{C \times H \times W}$ is the CAM input unit to compute the output channel attention $M_C \in R^{C \times 1 \times 1}$. It is increased by elements to get $F_1 \in R^{C \times H \times W}$, and F_1 is input to the SAM module. The spatial attention $M_D \in R^{1 \times H \times W}$ is produced utilizing an enlarged convolution with a dilated rate of 2 and kernel size of 3. At last, the number of channels is up-dimensioned to $R^{C \times H \times W}$ and then increased to get $F_2 \in R^{C \times H \times W}$ after the addition of spatial attention, as displayed in Eqs. (8) and (9).

$$M_D(F) = \sigma(f^{3 \times 3}_{dilat}([AvgPool(F); MaxPool(F)])) = \sigma(f^{3 \times 3}_{dilat}[F_{avg}^S; F_{max}^S]) \quad (8)$$

$$F_2 = M_D(F_1) \otimes F_1 \quad (9)$$

Where $f^{3 \times 3}_{dilat}$ represents a dilated convolution with a dilated rate of 2 and kernel size of 3.

To explore the current damage detection method with poor accuracy and extreme model parameters, EfficientNet is used as the support system to discover the model accuracy; DCBAM was developed to enhance EfficientNet feature learning of damage detection. EfficientNet is employed as the backbone to enhance accuracy in damage detection, with DCBAM enhancing feature learning to address poor accuracy and large model parameters in traditional methods.

First, the damaged image is exposed to pre-process operations like data enhancement, and the image is transformed into a fixed-size image to be trained $\in R^{3 \times 224 \times 224}$. After the initial phase of the down-sampling Conv process utilizing kernel sizes of $3 \times 3 \times 3$, the output is $S \in R^{40 \times 112 \times 112}$. At last, the FC layer is applied for damage recognition and classification, and the outcomes of micro-expression detection are attained. Table 1 describes the parameters of the DCBAM-EfficientNet model.

Parameter tuning using MSGO technique

At this stage, the MSGO approach is utilized for the optimal hyperparameter selection of the DCBAM-EfficientNet module²³. This approach is an advanced optimization technique inspired by the natural foraging behaviour of seagulls. It has exhibited significant merits in tuning DL methods because it can effectively search large and complex parameter spaces. Unlike conventional methods, MSGO balances exploration and exploitation well, which assists in avoiding local minima and ensuring global optimization. Its simplicity, ease of implementation, and capacity to adaptively refine solutions make it ideal for parameter tuning in DL methods. Compared to other techniques like genetic algorithms (GAs) or particle swarm optimization (PSO), MSGO converges faster and gives superior optimization accuracy, making it highly effective in enhancing model performance while maintaining computational efficiency. Figure 4 indicates the MSGO methodology.

This study employed the MSGO method, and the SOA method is further discussed in subsequent paragraphs.

Immigration

An immigration process mimics the movement of a seagull swarm into the position. This technique implements the exploration process.

(1) Updating the swarm location by adding the V parameter, as given below, prevents collision.

$$\vec{P} = V \times \vec{P}_c(i), i = 0, 1, 2, \dots, \text{Max}(i) \quad (10)$$

Stage i	Operator \widehat{F}_i	Resolution $(\widehat{H}_i \times \widehat{W}_i)$	#Channels \widehat{C}_i	#Layers \widehat{L}_i
1	Conv (3×3)	$224 \times 224 \times 40$	32	1
2	MBDConv1 (3×3)	$112 \times 112 \times 24$	16	1
3	MBDConv6 (3×3)	$56 \times 56 \times 32$	24	2
4	MBDConv6 (5×5)	$28 \times 28 \times 48$	40	2
5	MBDConv6 (3×3)	$14 \times 14 \times 96$	80	3
6	MBDConv6 (5×5)	$14 \times 14 \times 136$	112	3
7	MBDConv6 (5×5)	$14 \times 14 \times 232$	192	4
8	MBDConv6 (3×3)	$7 \times 7 \times 384$	320	1
9	Conv (1×1) Pooling FC	$7 \times 7 \times 1536$	1280	1

Table 1. Parameters of the DCBAM-EfficientNet model.

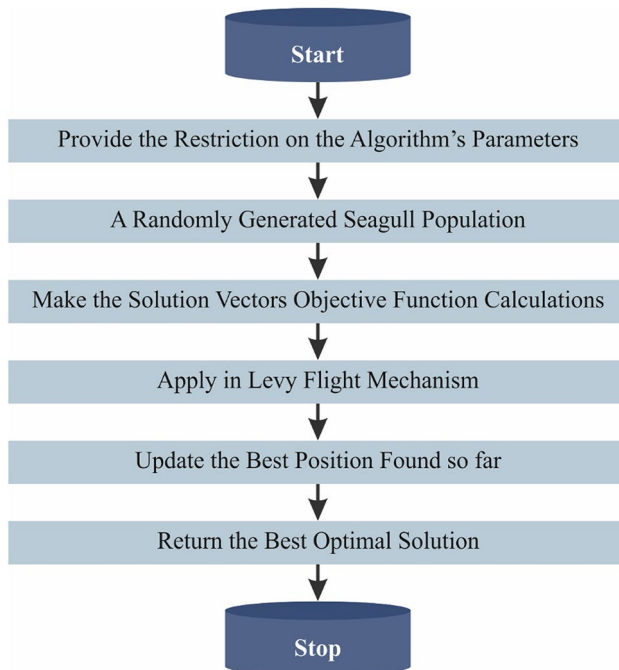


Fig. 4. Steps involved in the MSGO methodology.

In Eq. (10), $\vec{P}_c(i)$ indicates the location of the candidate in the existing iteration, \vec{P}_N denotes the location that stops it from interrelating with others, and V shows the dynamic performance of the candidate in the problem space and is shown in the following expression:

$$V = f_c - \left(i \times \left(\frac{f_c}{\text{Max}(i)} \right) \right) \quad (11)$$

In Eq. (11), i is the iteration, refers to the frequency management between 0 and f_c .

Equation (11) defines how the parameter V changes during successive rounds. The value of V is consistently lower as the iteration progresses, enabling the search candidate to explore the problem space comprehensively at the initial phase.

In the SOA, the immigration process exploits Eqs. (10), (11) to determine the updated location for the seagull candidate. The above equation ensures the candidate efficiently avoids collision and demonstrates exploratory behaviours during optimization. The method obtains a tradeoff between exploitation and exploration by adjusting its V value through the iteration number. Consequently, it conducts a search process to find the best solution.

II) While avoiding collision, the candidate approaches the best solution (optimum option) by exploiting the neighbours' information.

$$\vec{d} = K \times \left(\vec{P}_b(i) - \vec{P}_c(i) \right) \quad (12)$$

In Eq. (12), vector \vec{d}_e describes the relative placement of all the candidates ($\vec{P}_c(i)$) to the best-fitted candidate ($\vec{P}_b(i)$). The randomly selected coefficient K values control the ratio of exploitation to exploration.

$$K = 2 \times V^2 \times R \quad (13)$$

Here, R denotes the random integer within [0,1].

The calculation of K in Eq. (13) integrates a random component R and the motion behaviour parameter V . The K value influences how far the seagull candidate exploits the information from the best-fitted candidates rather than exploring the problem space. The SOA used to have a balance between exploitation and exploration by adjusting the K value. A high value of K promotes exploitation, which enables candidates to draw near the fittest solution. At the same time, a lower value of K prioritizes exploration, which allows the candidate to explore the alternate solution in the unexplored territory of the problem space.

III) The search agent gradually goes towards the fittest solution and modifies its location according to the optimum solution:

$$\vec{D}_e = \left| \vec{P}_N - \vec{d}_e \right| \quad (14)$$

In Eq. (14), \vec{D}_e denotes the difference between the ideal solution and the seagulls

The distance between the fittest or ideal solutions and the seagull candidates is evaluated in Eq. (14). The algorithm attains data about how much further each candidate is from the optimum solution by assessing these differences. The candidates modify the location to go towards the fittest solution progressively. The location modification of the candidate is implemented by minimizing the \vec{D}_e value. As the algorithm proceeds, the candidate's position is iteratively updated to reduce the discrepancy between the ideal solution and the existing locations. The SOA aims to gradually converge towards the fittest solutions by iteratively modifying the location of the search agent according to the most fitting solution.

Attacking

Seagulls keep changing their angle and velocity during migration and hold their positions in the flight through their feathers and mass. The exploitation process is performed in this stage. During the attack, individual seagulls migrate in a spiral pattern in the air along the y and z axis:

$$\hat{x} = r \times \cos(t) \quad (15)$$

$$\hat{y} = r \times \sin(t) \quad (16)$$

$$\hat{z} = r \times t \quad (17)$$

In the equation, t denotes the random integer within $[0, 2]$, and “ r ” is the value of the spiral turn radius.

$$r = \alpha \times e^{\beta T} \quad (18)$$

The spiral form is represented by α and β symbols, and “ e ” denotes the natural logarithm's base. The following equation is used to update the seagull location.

$$\vec{P}_c(i) = \left(\vec{D}_e \times \hat{x} \times \hat{y} \times \hat{z} \right) + \vec{P}_b(i) \quad (19)$$

In Eq. (19), $P_c(i)$ is the ideal result stored in vector.

The two main problems with SO are the convergence rate and early convergence. A solution is given to resolve these problems.

The modified SOA uses Lévy flight (LF) to increase the efficacy of SOA. This objective is to avoid the early convergence problems. The random walking features in LF contribute to dealing with the local search process:

$$Le(w) \approx w^{-1-\tau} \quad (20)$$

$$w = \frac{V}{|K|^{1/\tau}} \quad (21)$$

$$\sigma^2 = \left\{ \frac{\Gamma(1+\tau) \sin(\pi\tau/2)}{\tau \Gamma((1+\tau)/2) 2^{(1+\tau)/2}} \right\}^{\frac{2}{\tau}} \quad (22)$$

From the equations, $V \sim N(0, \sigma^2)$ and $K \sim N(0, \sigma^2)$, τ specifies the Levy index. Between 0 and 2 ($\tau = \frac{3}{2[26]}$), w implies the step size, $\Gamma(.)$ displays the Gamma function, and $V/K \sim N(0, 0.02)$ specifies that the samples were generated from the Gaussian distribution with variance of σ^2 and mean of 0, correspondingly.

Based on the approach above, the newly enhanced component is used to update the SOA solution:

$$\vec{D} = \vec{D} + \left| \vec{P} + \vec{d} \right| \times Le(\delta) \quad (23)$$

In Eq. (23), “ \vec{D}_{el} ” denotes the new position of the search candidate.

The best-fitted candidate is maintained by using Eq. (24) to arrive at the optimal solution for the candidate:

$$\vec{D} = \begin{cases} \vec{D}_{el} & F(\vec{D}_{el}) > F(\vec{D}_e) \\ \vec{D}_e & otherwise \end{cases} \quad (24)$$

This technique is used instead of traditional strategy to avoid getting trapped in the local minimal solution.

The MSGO methodology derives an FF to obtain higher classification efficiency. It determines a positive integer to characterize the more significant solution of the candidate's performance. Here, the decline of classifier errors is considered as FF.

$$\begin{aligned} \text{fitness}(x_i) &= \text{ClassifierErrorRate}(x_i) \\ &= \frac{\text{No. of misclassified samples}}{\text{Total No. of samples}} \times 100 \end{aligned} \quad (25)$$

Ensemble learning

Finally, an ensemble of three models, namely LSTM, BiGRU, and SAE, is implemented to classify and detect the damages. The ensemble models are chosen due to their complementary merits in handling sequential data and capturing complex patterns. LSTM is ideal for learning long-term dependencies in time-series data, making it appropriate for tasks with significant temporal relationships. BiGRU improves this by giving bidirectional processing, allowing the model to learn from past and future contexts in the sequence. On the contrary, SAE is effectual for dimensionality reduction and feature extraction, ensuring that the model captures key structural data without losing critical details. By incorporating these models, the ensemble maximizes robustness, enhances generalization across diverse damage patterns, and improves accuracy compared to individual models. This multi-model approach enhances overall performance in detecting complex damage scenarios while mitigating overfitting and improving model resilience.

LSTM model

The LSTM is an RNN method capable of resolving the explosion and disappearance gradient issues. The longer-time sequence procedure is planned to prevent the longer-term dependence issue²⁴. When equated with the usual RNN method, the LSTM technique can achieve enhancement in a long-time sequence. The hidden layer (HL) of the new RNN contains a single state; therefore, it is challenging to provide short-term input. Dual outputs are accessible, such as the cell state at the present moment C_t and the output value at the present moment h_t . Figure 5 demonstrates the framework of LSTM.

LSTM executes this method over 3 gate devices: forget, input, and output. The input and output gates have been utilized to obtain output and precise parameters. The forget gate limits how many cell states of the prior time step C_{t-1} are taken to the cell state of the present moment C_t .

$$f_t = \sigma(W_f \otimes (X_t h_{t-1}) + b_f) \# () \quad (26)$$

Whereas \otimes signifies the dot multiplication. $\sigma(\cdot)$ denotes the sigmoid function. Then, compute the values of input gate i_t and candidate state \tilde{C}_t at moment t :

$$i_t = \sigma(W_i \otimes (X_t h_{t-1}) + b_i) \quad (27)$$

$$\tilde{C}_t = \sigma(W_c \otimes (X_t h_{t-1}) + b_c) \neq () \quad (28)$$

The upgraded value \tilde{C}_t of the cell layer below the present time t is gained from the above calculation:

$$C_t = f_t \otimes C_{t-1} + i_t \otimes \tilde{C}_t \neq () \quad (29)$$

Lastly, estimate the present output value of the output gate as per the upgrade value of the cell state at present t :

$$O_t = \sigma(W_o \otimes (X_t h_{t-1}) + b_o) \quad (30)$$

$$h_t = O_t \otimes \tanh(C_t) \# () \quad (31)$$

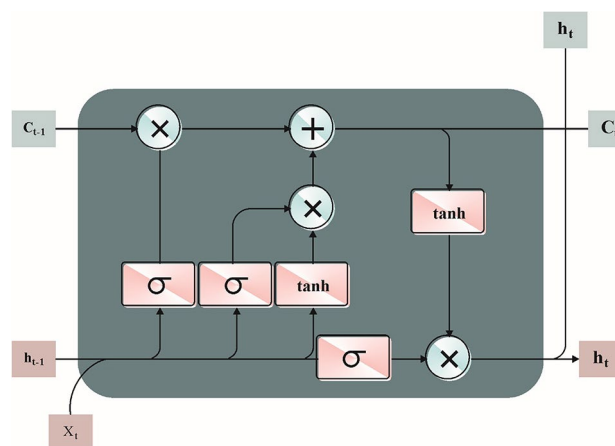


Fig. 5. LSTM architecture.

BiGRU model

GRU is an overview of the LSTM technique. The LSTM method efficiently improves the issue of gradient vanishing compared to the usual RNN method. The GRU reshapes the interior structure of the LSTM dependent upon the gating concept, thus decreasing the training complexity and computational time. Like the LSTM method, for an input series $\{x_1, x_2, x_3, \dots, x_t, \dots x_n\}$, the GRU can successively attain its HL h_t at time step t as per Eqs. (30), (31), (32), (33):

$$r_t = \sigma(W_r x_t + b_r + W_{hr} h_{t-1} + b_{hr}) \# () \quad (32)$$

$$z_t = \sigma(W_z x_t + b_z + W_{hz} h_{t-1} + b_{hz}) \# () \quad (33)$$

$$n_t = \tanh(W_n x_t + b_n + r_t \otimes (W_{hn} h_{t-1} + b_{hn})) \# () \quad (34)$$

$$h_t = (1 - z_t) \otimes n_t + z_t \otimes h_{t-1} \neq () \quad (35)$$

Whereas h_{t-1} is the HL of time step $t - 1$; $\sigma(\cdot)$ denotes the sigmoid function, b specifies the bias term, r_t , z_t , and n_t refers to the gated state upgraded at every time step t . Bi-GRU forms dual reverse GRU methods simultaneously, forming time sequence information forward and backwards.

SAE model

The AE comprises the encoding and decoding parts²⁵. During the encoder process, it converts the original features into hidden depictions and recreates the hidden representation into relevant features during the decoder process.

An encoder function f is used to map the input dataset $x \in \mathbb{R}^m$ into low-dimensional hidden feature space \mathbb{R}^n :

$$h = f(x) = \phi(W_1^T x + b_1) \quad (36)$$

In Eq. (36), W_1^T refers to the weight matrix (W) transformed among the HL and input layers, ϕ denotes the activation function, b_1 is a bias, and h indicates the hidden vector of the latent layer. The decoder function g map h is used to reconstruct feature x' . It is formulated by Eq. (37):

$$x' = g(x) = \phi(W_2^T h + b_2) \quad (37)$$

W_2^T indicates the weight matrix (W) between output layers and HLs, and b_2 is a bias.

$$\min_{\theta} J_{AE}(\theta) = \frac{1}{2n} \sum_{i=1}^n \|x_i - x'_i\|^2 \quad (38)$$

In Eq. (38), J_{AE} refers to the reconstructed loss of AE, and n shows the number of input samples. The structure of SAE is based on AE. While recreating the input, the distribution of recreated features has numerous overlaps due to over-fitting problems, and copying the input might not characterize essential data. To resolve these challenges, a sparse constraint term is added as a penalty term that suppresses the neuron output once the amount of neurons in the HL is more significant and expressed as in Eq. (39):

$$\min_{\theta} J_{SAE}(\theta) = \frac{1}{n} \sum_{i=1}^n \|x_i - x'_i\|^2 + \epsilon \sum_{j=1}^s KL(\rho || \hat{\rho}_j) \quad (39)$$

KL divergence measures discrepancies among two probability distributions. s implies the number of neurons in the HL, J_{SAE} indicates the objective of SAE, ρ denotes the sparse parameter, and $\hat{\rho}_j$ denotes the activation probability.

Result analysis and discussion

The experimental evaluation of the ADD-MSGOEL method is examined using the CODEBRIM dataset²⁶ (<https://zenodo.org/records/2620293>), which comprises 10,850 samples with six classes as defined in Table 2. Figure 6 represents the sample images.

Figure 7 defines the confusion matrices produced by the ADD-MSGOEL technique at 80%:20% and 70%:30% of TRAPS/TESPS. The outcomes stated the effective detection and classification of six classes.

Table 3 highlights the overall damage detection result of the ADD-MSGOEL technique on 80%:20% of TRAPS/TESPS. Figure 8 presents an average analysis of the ADD-MSGOEL technique on 80% of TRAPS. The figure highlighted that the ADD-MSGOEL technique reaches effectual detection of no defect and various kinds of defects. With 80%TRAPS, the ADD-MSGOEL method provides an average $accu_y$ of 97.59%, $prec_n$ of 92.55%, $reca_l$ of 91.29%, and F_{score} of 91.85%.

An average analysis of the ADD-MSGOEL technique on 20% of TESPS is shown in Fig. 9. The experimental value indicated that the ADD-MSGOEL method obtains effective detection of defects. With 20% of TESPS, the ADD-MSGOEL method provides an average $accu_y$ of 97.45%, $prec_n$ of 91.94%, $reca_l$ of 90.88%, and F_{score} of 91.35%.

The overall damage detection outcomes of the ADD-MSGOEL technique on 70%:30% of TRAPS/TESPS are depicted in Table 4. An average analysis of the ADD-MSGOEL technique on 70% of TRAPS is presented in

Classes	No. of samples
“No defect (background)”	2506
“Corrosion (stains)”	1599
“Crack”	2507
“Efflorescence”	833
“Exposed Bars”	1507
“Spallation”	1898
Total samples	10,850

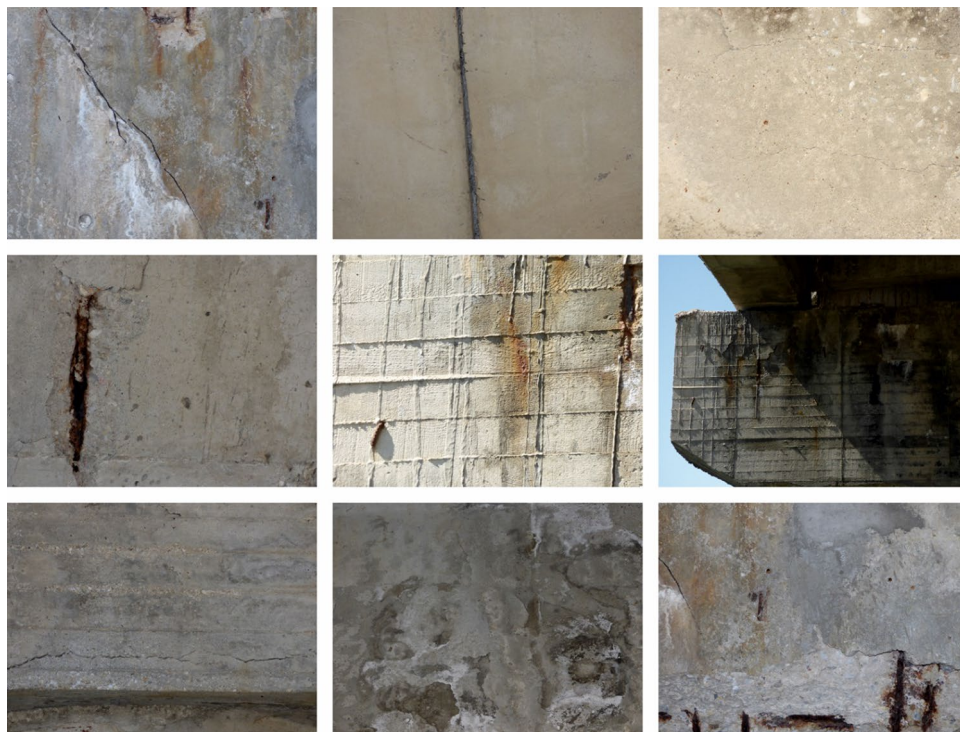
Table 2. Details on database.**Fig. 6.** Sample images.

Fig. 10. The experimental value inferred that the ADD-MSGOEL method obtains effective recognition detection of defects. With 80% TRAPS, the ADD-MSGOEL method attains an average $accu_y$ of 96.15%, $prec_n$ of 88.29%, $reca_l$ of 86.45%, and F_{score} of 87.23%.

An average analysis of the ADD-MSGOEL technique on 30% of TESPS is illustrated in Fig. 11. The figure highlighted that the ADD-MSGOEL method obtains effective detection of defects. With 20% of TESPS, the ADD-MSGOEL method obtains an average $accu_y$ of 96.45%, $prec_n$ of 88.79%, $reca_l$ of 87.71%, and F_{score} of 88.19%.

The $accu_y$ outcome for training (TRA) and validation (VL) provided in Fig. 12 for the ADD-MSGOEL methodology at 80%:20% of TRAPS/TEPS offers an appreciated vision of its performance under different epochs. Mainly, there is a consistent improvement in TRA and TES $accu_y$ to maximal epochs, representing the model's ability to learn and recognize patterns from both data.

Figure 13 presents a comprehensive overview of TRA and TES loss outcomes for the ADD-MSGOEL method at 80%:20% of TRAPS/TEPS over dissimilar epochs. The TRA loss constantly decreases as the model increases weights to decrease classifier errors on both databases. The loss curves portray the model's configuration with the TRA database, emphasizing its ability to capture both data effectively.

The findings confirm that the ADD-MSGOEL under 80:20% of TRAPS/TEPS continuously obtains maximum PR outcome across all the classes concerning the PR outcome given in Fig. 14. This experimental value highlights the simulation's capability to discriminate between 6 classes, the importance of its efficacy in detecting class labels.

Furthermore, in Fig. 15, ROC curves generated by the ADD-MSGOEL at 80%:20% of TRAPS/TEPS are presented, representing its aptitude to differentiate among six classes. The outcomes emphasize the model's classification performance on six classes, highlighting its effectiveness in addressing the classifier problem.

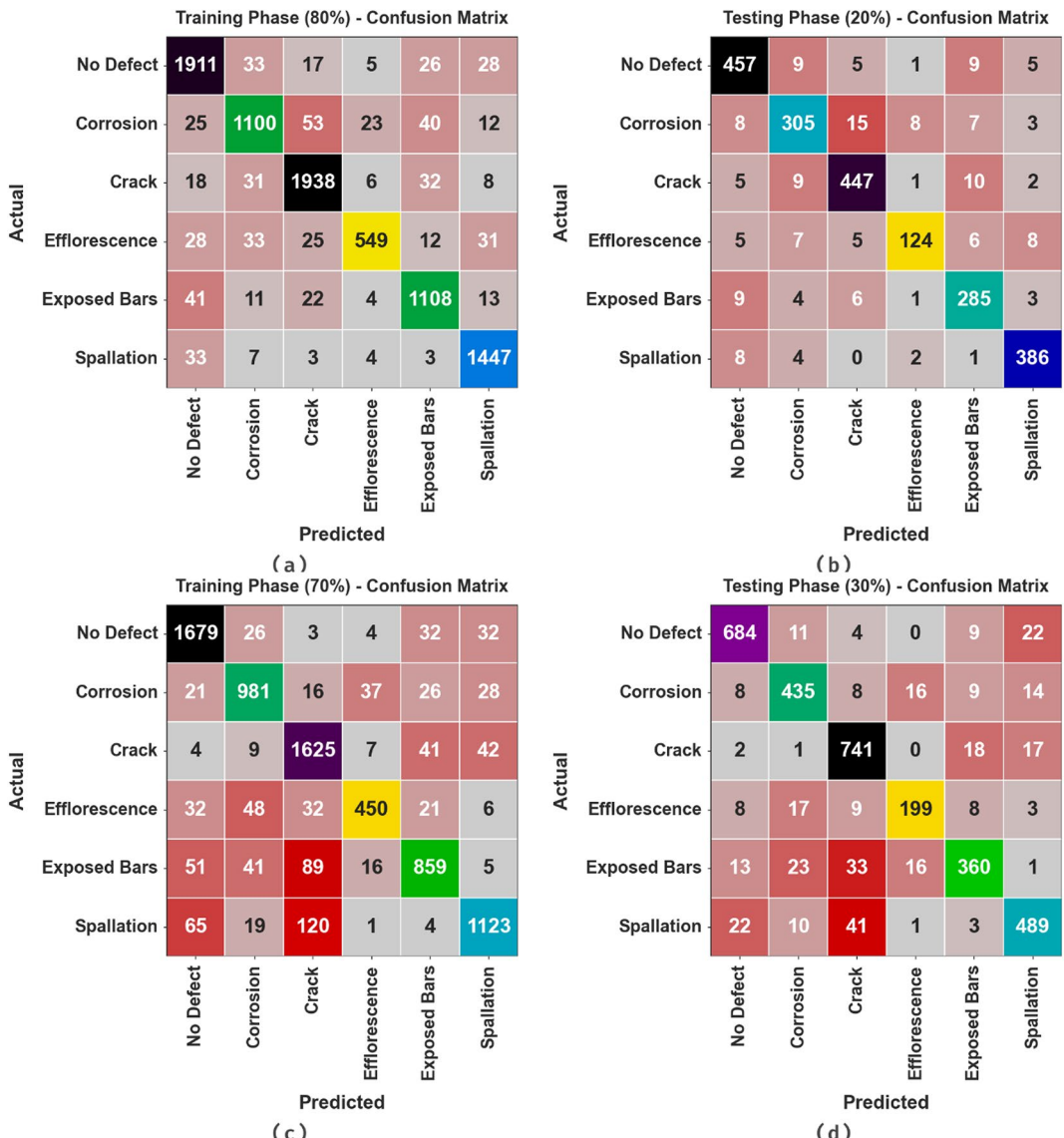


Fig. 7. Confusion matrices of (a,b) 80:20% of TRAPS/TEPS and (c,d) 70:30% of TRAPS/TEPS.

In Fig. 16, the comparative results of the ADD-MSGOEL technique with recent models are portrayed²⁷. The results highlighted that the MetaQNN and ENAS approaches have reported the lowest performance. Simultaneously, the VGG16 and Inceptionv3 approaches have obtained enhanced outcomes. Meanwhile, the ResNet50, Xception, and RCBDD-AODAFF approaches have performed considerably. However, the ADD-MSGOEL technique demonstrates more excellent performance with maximum $accu_y$, $prec_n$, and $recal$ of 97.59%, 92.55%, and 91.29%, correspondingly.

Figure 17 depicts the comparative computational time (CT) outcomes of the ADD-MSGOEL methodology with existing techniques. The outcomes emphasize that the MetaQNN and ENAS models have reported the lowest performance. Simultaneously, the VGG16 and Inceptionv3 techniques have attained certainly superior outcomes. Meanwhile, the ResNet50, Xception, and RCBDD-AODAFF approaches have performed excellently. However, the ADD-MSGOEL method depicts superior performance with a minimum CT of 0.91s.

From the extensive comparative results, it is apparent that the ADD-MSGOEL technique gains effectual detection of damages.

Conclusion

In this study, the ADD-MSGOEL approach for visually impaired people is presented. The ADD-MSGOEL approach is designed to enhance the social life and daily functioning of visually impaired people by accurately detecting damage and potential hazards in their surroundings. In the primary stage, the ADD-MSGOEL model follows a CLAHE-based CLAHE approach to increase the image's quality. Next, the features are extracted using the DCBAM-EfficientNet Module, which derives the complex and intrinsic features. Moreover, the MSGO model is employed to choose the optimal parameter for the DCBAM-EfficientNet Module. At last, an ensemble of three

Classes	Accu _y	Prec _n	Reca _l	F _{Score}
TRAPS (80%)				
No Defect	97.07	92.95	94.60	93.77
Corrosion	96.91	90.53	87.79	89.14
Crack	97.52	94.17	95.33	94.74
Efflorescence	98.03	92.89	80.97	86.52
Exposed Bars	97.65	90.75	92.41	91.57
Spallation	98.36	94.02	96.66	95.32
Average	97.59	92.55	91.29	91.85
TESPS (20%)				
No Defect	97.05	92.89	94.03	93.46
Corrosion	96.59	90.24	88.15	89.18
Crack	97.33	93.51	94.30	93.91
Efflorescence	97.97	90.51	80.00	84.93
Exposed Bars	97.42	89.62	92.53	91.05
Spallation	98.34	94.84	96.26	95.54
Average	97.45	91.94	90.88	91.35

Table 3. Damage detection outcome of ADD-MSGOEL technique at 80:20% of TRAPS/TESPS. Significant values are given in bold.

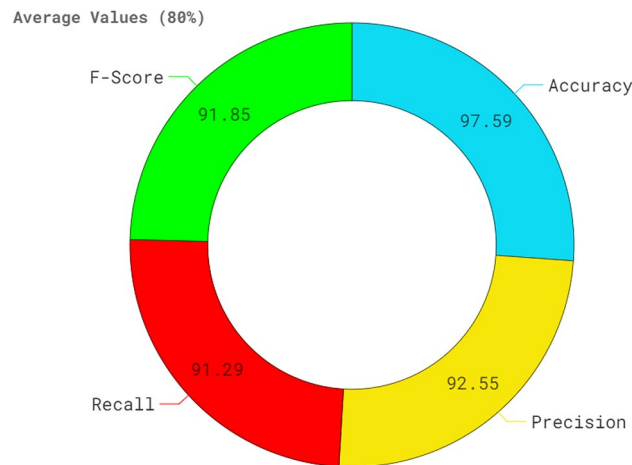


Fig. 8. Average outcome of ADD-MSGOEL technique at 80% of TRAPS.

models, namely LSTM, BiGRU, and SAE, is utilized to classify and detect the damages. To demonstrate the effectiveness of the ADD-MSGOEL technique, a series of experiments were conducted using the CODEBRIM dataset. The experimental validation of the ADD-MSGOEL technique portrayed a superior accuracy value of 97.59% over existing models.

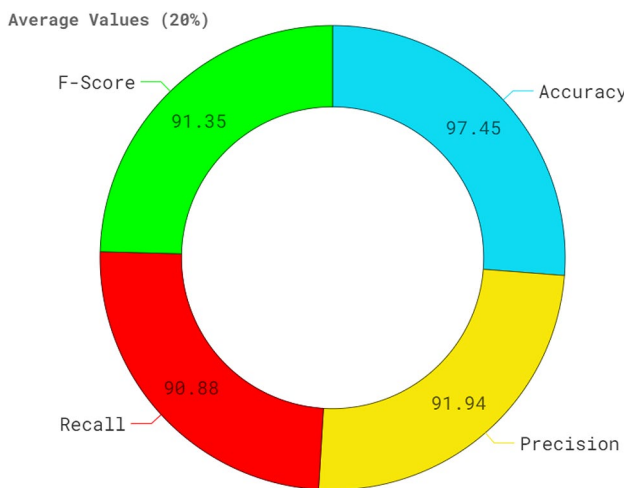


Fig. 9. Average outcome of ADD-MSGOEL technique at 20% of TESPS.

Classes	Accu _y	Prec _n	Reca _t	F _{Score}
TRAPS (70%)				
No defect	96.45	90.66	94.54	92.56
Corrosion	96.43	87.28	88.46	87.86
Crack	95.22	86.21	94.04	89.95
Efflorescence	97.31	87.38	76.40	81.52
Exposed bars	95.71	87.39	80.96	84.05
Spallation	95.76	90.86	84.31	87.46
Average	96.15	88.29	86.45	87.23
TESPS (30%)				
No defect	96.96	92.81	93.70	93.25
Corrosion	96.41	87.53	88.78	88.15
Crack	95.91	88.64	95.12	91.76
Efflorescence	97.60	85.78	81.56	83.61
Exposed bars	95.91	88.45	80.72	84.41
Spallation	95.88	89.56	86.40	87.95
Average	96.45	88.79	87.71	88.19

Table 4. Damage detection outcome of ADD-MSGOEL technique at 70%:30% of TRAPS/TEPS. Significant values are given in bold.

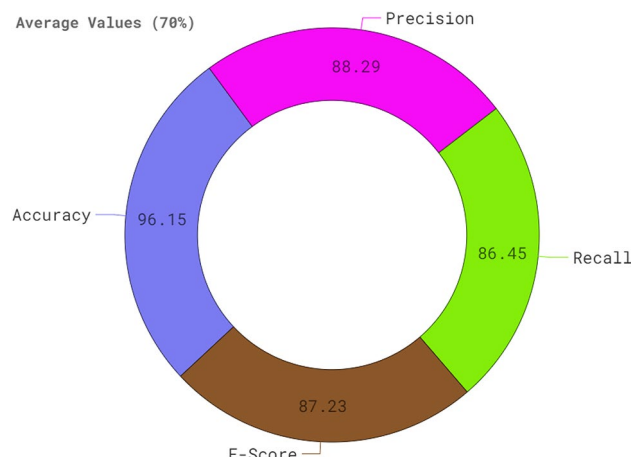


Fig. 10. Average outcome of ADD-MSGOEL technique at 70% of TRAPS.

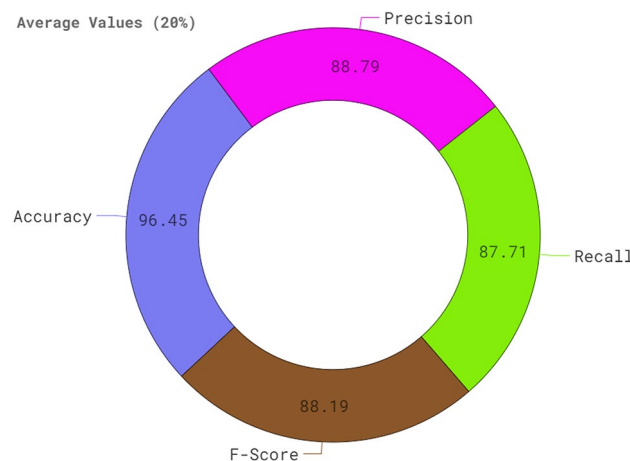


Fig. 11. Average outcome of ADD-MSGOEL technique at 30% of TESPS.

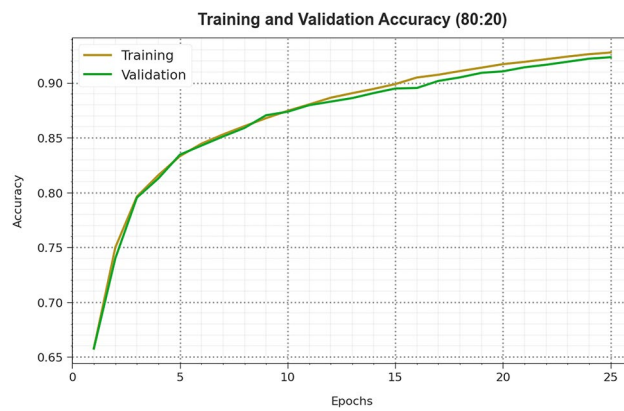


Fig. 12. $Accu_y$ curve of ADD-MSGOEL technique at 80%:20% of TRAPS/TEPS.

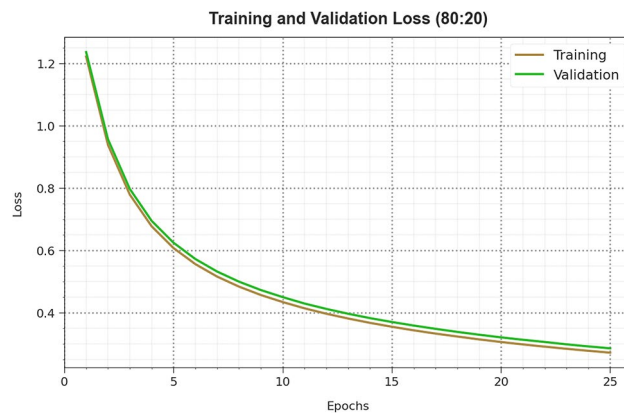


Fig. 13. Loss curve of ADD-MSGOEL methodology at 80:20% of TRAPS/TEPS.

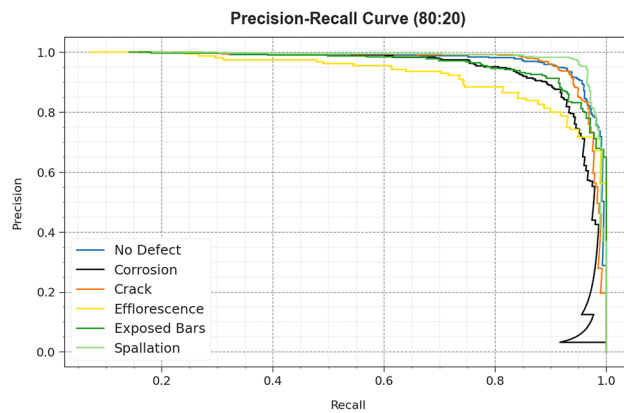


Fig. 14. PR curve of ADD-MSGOEL technique under 80%:20% of TRAPS/TESPS.

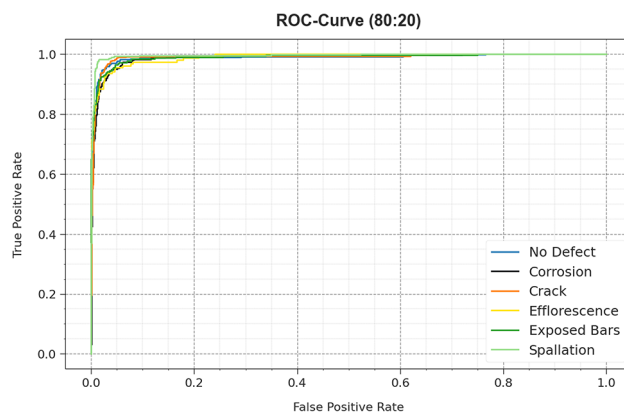


Fig. 15. ROC curve of ADD-MSGOEL approach at 80%:20% of TRAPS/TESPS.

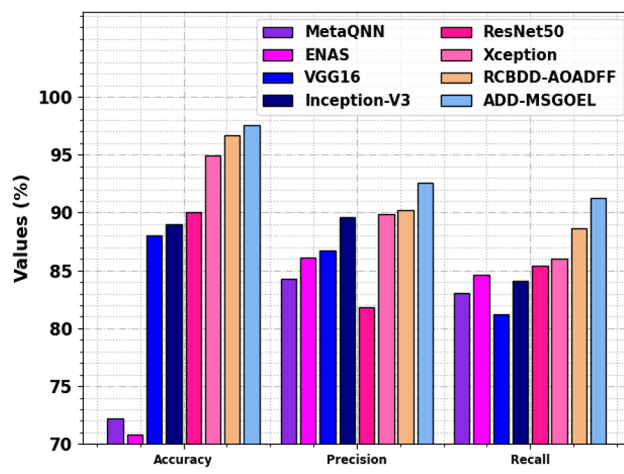


Fig. 16. Comparative analysis of ADD-MSGOEL technique with recent models.

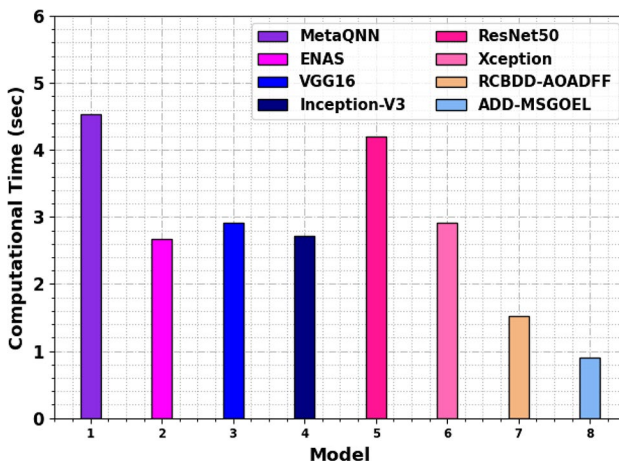


Fig. 17. CT analysis of ADD-MSGOEL technique with recent models.

Data availability

The authors confirm that the data supporting this study's findings are available within the article: Mundt M, Majumder S, Murali S, Panetsos P, Ramesh V. Meta-learning Convolutional Neural Architectures for Multi-target Concrete Defect Classification with the COncrete DEfect BRidge IMage Dataset. Apr. 2019.

Received: 1 December 2024; Accepted: 23 April 2025

Published online: 13 May 2025

References

- Chen, L. et al. Convolutional neural networks (CNNs)-based multi-category damage detection and recognition of high-speed rail (HSR) reinforced concrete (RC) bridges using test images. *Eng. Struct.* **276**, 115306 (2023).
- Prashar, D., Chakraborty, G. & Jha, S. Energy efficient laser based embedded system for blind turn traffic control. *J. Cybersecur. Inform. Manag.* **2** (2), 35–43 (2020).
- Cavaleri, L. et al. Convolution-based ensemble learning algorithms to estimate the bond strength of the corroded reinforced concrete. *Constr. Build. Mater.* **359**, 129504 (2022).
- Inam, H., Islam, N. U., Akram, M. U. & Ullah, F. Smart and automated infrastructure management: A deep learning approach for crack detection in Bridge images. *Sustainability* **15** (3), 1866 (2023).
- Ai, L., Soltangharaei, V. & Ziehl, P. Developing a heterogeneous ensemble learning framework to evaluate Alkali-silica reaction damage in concrete using acoustic emission signals. *Mech. Syst. Signal Process.* **172**, 108981 (2022).
- Ai, D. & Cheng, J. A deep learning approach for electromechanical impedance-based concrete structural damage quantification using a two-dimensional convolutional neural network. *Mech. Syst. Signal Process.* **183**, 109634 (2023).
- Zoubir, H., Rguig, M. & Elaroussi, M. Crack recognition automation in concrete bridges using Deep Convolutional Neural Networks. In *MATEC Web of Conferences*. EDP Sciences, 03014. (2021).
- Svendsen, B. T., Froseth, G. T., Øiseth, O. & Rønquist, A. A data-based structural health monitoring approach for damage detection in steel bridges using experimental data. *J. Civil Struct. Health Monit.* **1**–15. (2022).
- Pennada, S., Perry, M., McAlorum, J., Dow, H. & Dobie, G. Threshold-based BRISQUE-assisted deep learning for enhancing crack detection in concrete structures. *J. Imaging.* **9** (10), 218 (2023).
- Lee, K., Jeong, S., Sim, S. H. & Shin, D. H. Damage-Detection approach for bridges with Multi-Vehicle loads using convolutional autoencoder. *Sensors* **22** (5), 1839 (2022).
- Asghari, A., Ghodrati Amiri, G., Darvishan, E. & Asghari, A. A novel approach for structural damage detection using Multi-Headed stacked deep ensemble learning. *J. Vib. Eng. Technol.* **1**–16. (2023).
- Mohammed Abdolkader, E., Moselhi, O., Marzouk, M. & Zayed, T. Entropy-based automated method for detection and assessment of spalling severities in reinforced concrete bridges. *J. Perform. Constr. Facil.* **35** (1), 04020132 (2021).
- Hong, S. S., Hwang, C. H., Chung, S. W. & Kim, B. K. A Deep-Learning-Based Bridge damaged object automatic detection model using a Bridge member model combination framework. *Appl. Sci.* **12** (24), 12868 (2022).
- Han, Q., Ma, Q., Dang, D. & Xu, J. Modal Parameters Prediction and Damage Detection of Space Grid Structure under Environmental Effects Using Stacked Ensemble Learning. *Struct. Control Health Monit.* **2023**. (2023).
- Zhang, Q., Barri, K., Babanajad, S. K. & Alavi, A. H. Real-time detection of cracks on concrete Bridge decks using deep learning in the frequency domain. *Engineering* **7** (12), 1786–1796 (2021).
- Mousavi, A. A., Zhang, C., Masri, S. F. & Gholipour, G. Damage detection and characterization of a scaled model steel truss Bridge using combined complete ensemble empirical mode decomposition with adaptive noise and multiple signal classification approach. *Struct. Health Monit.* **21** (4), 1833–1848 (2022).
- Laxman, K. C., Tabassum, N., Ai, L., Cole, C. & Ziehl, P. Automated crack detection and crack depth prediction for reinforced concrete structures using deep learning. *Constr. Build. Mater.* **370**, 130709 (2023).
- Fernandez-Navamuel, A. et al. Supervised deep learning with finite element simulations for damage identification in bridges. *Eng. Struct.* **257**, 114016 (2022).
- Atitallah, A. B. et al. An effective obstacle detection system using deep learning advantages to aid blind and visually impaired navigation. *Ain Shams Eng. J.* **15** (2), 102387 (2024).
- Wu, Y. et al. Overhead power line damage detection: an innovative approach using enhanced YOLOv8. *Electronics* **13** (4), 739 (2024).
- Sarki, R. et al. Image pre-processing in classification and identification of diabetic eye diseases. *Data Sci. Eng.* **6** (4), 455–471 (2021).

22. Qi, F., Yang, C., Shi, B. & Ma, S. Micro-expression recognition based on DCBAM-EfficientNet model. *J. Phys. Conf. Ser.* **2504** (1), 012062 (2023).
23. Wang, Q., Zhang, M. & Abdolhosseinzadeh, S. Application of modified seagull optimization algorithm with archives in urban water distribution networks: dealing with the consequences of sudden pollution load. *Heliyon*, e24920. (2024).
24. Zhao, L., Luo, T., Jiang, X. & Zhang, B. Prediction of soil moisture using BiGRU-LSTM model with STL decomposition in Qinghai-Tibet plateau. *PeerJ* **11**, e15851 (2023).
25. Lee, H., Hur, C., Ibrokhimov, B. & Kang, S. Interactive guiding sparse Auto-Encoder with Wasserstein regularization for efficient classification. *Appl. Sci.* **13** (12), 7055 (2023).
26. Mundt, M., Majumder, S., Murali, S., Panetsos, P. & Ramesh, V. Meta-learning Convolutional Neural Architectures for Multi-target Concrete Defect Classification with the COncrete DEfect BRidge IMage Dataset. (2019).
27. Eltahir, M. M., Aldehim, G., Almalki, N. S., Alnfaai, M. M. & Osman, A. E. Reinforced concrete Bridge damage detection using arithmetic optimization algorithm with deep feature fusion. *AIMS Math.* **8** (12), 29290–29306 (2023).

Acknowledgements

The authors extend their appreciation to the King Salman center For Disability Research for funding this work through Research Group no KSRG-2024- 127.

Author contributions

Sana Alazwari: Conceptualization, methodology, validation, investigation, writing—original draft preparation, funding; Hussah Nasser AlEisa: Conceptualization, methodology, writing—original draft preparation, writing—review and editing; Mohammed Rizwanullah: methodology, validation, writing—original draft preparation; Radwa Marzouk: software, validation, data curation, writing—review and editing.

Declarations

Competing interests

The authors declare no competing interests.

Additional information

Correspondence and requests for materials should be addressed to S.A.

Reprints and permissions information is available at www.nature.com/reprints.

Publisher's note Springer Nature remains neutral with regard to jurisdictional claims in published maps and institutional affiliations.

Open Access This article is licensed under a Creative Commons Attribution-NonCommercial-NoDerivatives 4.0 International License, which permits any non-commercial use, sharing, distribution and reproduction in any medium or format, as long as you give appropriate credit to the original author(s) and the source, provide a link to the Creative Commons licence, and indicate if you modified the licensed material. You do not have permission under this licence to share adapted material derived from this article or parts of it. The images or other third party material in this article are included in the article's Creative Commons licence, unless indicated otherwise in a credit line to the material. If material is not included in the article's Creative Commons licence and your intended use is not permitted by statutory regulation or exceeds the permitted use, you will need to obtain permission directly from the copyright holder. To view a copy of this licence, visit <http://creativecommons.org/licenses/by-nc-nd/4.0/>.

© The Author(s) 2025